

Exploring the Icy World of the Edgeworth-Kuiper Belt – An ESO Large Programme

- H. BOEHNHARDT (*Max-Planck-Institut für Astronomie, Heidelberg, Germany*)
A. BARUCCI, A. DELSANTI, C. DE BERGH, A. DORESSOUNDIRAM, J. ROMON
(*Observatoire de Paris, Meudon, France*)
E. DOTTO (*Osservatorio Astronomico di Roma, Italy*)
G. TOZZI (*Osservatorio Astronomico di Arcetri, Firenze, Italy*)
M. LAZZARIN, S. FOURNISIER (*Osservatorio Astronomico di Padova, Italy*)
N. PEIXINHO (*Observatorio Astronomico de Lisboa, Portugal, and Observatoire de Paris, Meudon, France*)
O. HAINAUT (*European Southern Observatory, Santiago de Chile*)
J. DAVIES (*Royal Observatory Edinburgh, Great Britain*)
P. ROUSSELOT (*Observatoire de Besançon, France*)
L. BARRERA (*Universidad Católica del Norte, Antofagasta, Chile*)
K. BIRKLE (*Max-Planck-Institut für Astronomie, Heidelberg, Germany*)
K. MEECH (*University of Hawaii, Honolulu, USA*)
J. ORTIZ (*Instituto de Astronomia de Andalucía, Granada, Spain*)
T. SEKIGUCHI, J.-I. WATANABE (*National Astronomical Observatory, Mitaka-Tokyo, Japan*)
N. THOMAS (*Max-Planck-Institut für Aeronomie, Katlenburg-Lindau, Germany*)
R. WEST (*European Southern Observatory, Garching, Germany*)

The Edgeworth-Kuiper Belt and the Formation of the Solar System

The first object in the Edgeworth-Kuiper Belt was observed in 1930, when Clyde Tombaugh discovered Pluto at a distance of 43 AU (1 AU = one astronomical unit, the mean distance between Earth and the Sun = 149.6 million km), i.e. beyond the orbit of Neptune. About 20 years later Edgeworth and Kuiper started to speculate about the existence of another asteroid belt at the edge of the planetary system. Another 30 years later this speculation became an hypothesis when Fernandez and Ip argued for the existence of an Ecliptic-oriented reservoir of icy bodies beyond Neptune as a source for short-period comets, the recruitment of which was difficult to explain by gravitational capturing of Oort Cloud comets through planets when approaching the inner solar system. The hypothesis became reality in 1992, when, during a search campaign for distant asteroids, Jewitt and Luu found 1992 QB₁ (now numbered: 15760) at a distance of 41 AU from the Sun.

In the meanwhile, after the detection of more than 700 objects beyond the orbit of Neptune over the past decade, a new class of solar system bodies has been discovered. These Transneptunian Objects (TNOs) are the largest members of the Edgeworth-Kuiper Belt. They have caused a complete revision of our knowledge and understanding of the outer solar system: the Edgeworth-

Kuiper Belt is believed to represent the most original remnant from the formation period of our planetary system. It was in this region where within less than 20 million years some 4.6 billion years ago, icy planetesimals formed and grew to larger bodies, nowadays observed as TNOs, Centaurs, short-period comets and some icy satellites of the major planets. Although of the same origin and most likely containing the same primordial material, these small bodies, as we observe them now, have experienced different evolution over the age of the solar system, both dynamically and physically. Nevertheless, they contain the most primordial material from the formation of the Sun and its planetary system that we can observe today.

The Global View of the Edgeworth-Kuiper Belt and its Population of Objects

The dynamical ‘zoo’ of Cubewanos, Plutinos, Centaurs and SDOs: According to current dynamical scenarios, the TNO population remained in the region of its formation, the Edgeworth-Kuiper Belt, over the age of the solar system. However, their orbits became perturbed by the presence of Neptune. The gravitational interaction with this giant planet has ‘pumped’ objects into so-called ‘excited’ (i.e. non-circular and/or inclined), but non-resonant orbits creating the dynamical class of ‘Cubewanos’ (named after the prototype object 1992 QB₁), also called clas-

sical disk objects. Other TNOs were captured in resonant orbits with Neptune forming the dynamical class of ‘Plutinos’ (named after Pluto, the most prominent representative in the 3:2 resonance orbit). Gravitational scattering at Neptune has produced the class of ‘Scattered Disk Objects (SDOs)’ in very eccentric orbits with semi-major axes between 50 and several 1000 AU. The ‘Centaurs’, presently in orbits between Neptune and Jupiter and named after half-human-half-horse demigods in Greek mythology, are also considered to be scattered TNOs, cascading towards the Sun by repeated gravitational interaction with the major planets. At the end, i.e. typically after some 10 million years in intermediate orbits, Jupiter will either capture them as short-period comets (thus, some of them even become accessible for spacecraft exploration) or will expel them into the region of the long-period Oort Cloud or even interstellar comets at the edge of the solar system. A few TNOs may get stranded as satellites around the outer gas giants (the most prominent candidate is Triton, the largest moon of Neptune).

The original formation disk, more ‘Plutos’ and TNO binaries: The drop in the number of objects with semi-major axes larger than 50 AU may indicate either a basic characteristic of the formation disk around our Sun (a ‘truncated’ disk?) or may just mark the challenge to detect the ‘cold’ and very collimated formation disk of even smaller planetesimals that escaped the gravita-

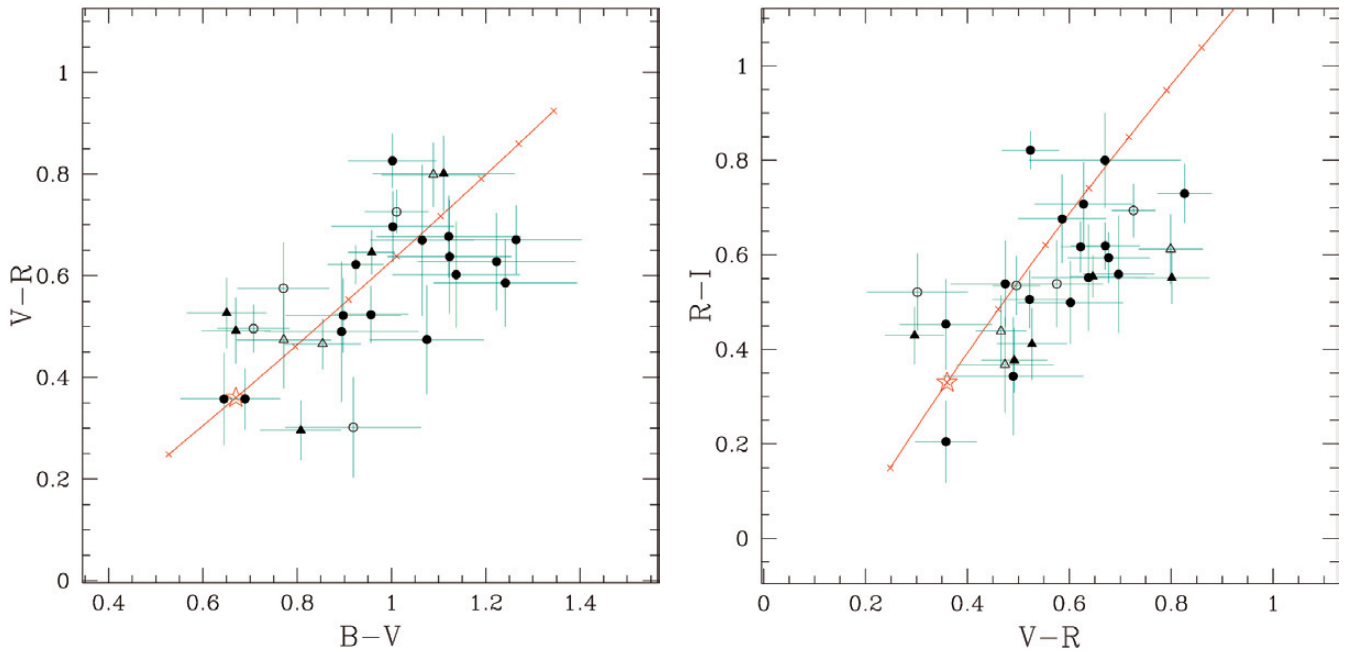


Figure 1: Colour-colour diagrams of the first 28 objects observed within the Large Programme. The two panels show the B-V versus V-R (left) and R-I versus V-R (right) colours of the objects measured. The symbols are: filled circles = Cubewanos, filled triangles = Plutinos, open circles = SDOs, open triangles = Centaurs. The colour of the Sun is indicated by the open star symbol. The lines indicate the direction of increasing reddening slopes from -10 (lower left end) to $70\%/100$ nm (upper right end) in steps of $10\%/100$ nm. The distribution of the measured objects seems to be rather uniform in the typical reddening range. The shift of the objects below the line of constant reddening in the plots involving R-I colour is due to the spectral slope change of red objects towards the near-IR end of the visible spectrum.

tional influence of the outermost planets because of their large distance from the Sun. The overall mass in the Edgeworth-Kuiper Belt seems to be very small (0.15 Earth masses) and cannot explain the existence of large TNOs like Pluto/Charon or Varuna. Instead modelling results suggest that the original formation disk in the TNO region was much heavier (10–100 Earth masses), that it should have produced more Pluto-size bodies and that most of its mass got lost by gravitational scattering at the large planets as well as by mutual collisions of TNOs and subsequent down-grinding of the colli-

sion products to micron size dust that the solar radiation pressure has removed from the Edgeworth-Kuiper Belt region. The existence of binary TNOs (about 10 objects so far) supports the idea of a serious collision environment in the belt during and possibly beyond the end of the formation period of planetesimals. Ongoing search programmes using imaging surveys and high-resolution imaging techniques at large telescopes world-wide try to solve these key questions on the Edgeworth-Kuiper Belt.

Physico-chemical properties: While the dynamical history of TNOs

and their relatives seems to be reasonably well understood, just a very vague picture of their physical properties and chemical constitution exists. The faintness of the objects (the vast majority are fainter than 23 mag) makes them difficult to observe even with the largest telescopes: the brightest representatives (about 20 mag) require easily one full observing night at an 8-m VLT unit telescope for a spectroscopic study of decent signal-to-noise.

Despite their faintness, the observed TNOs and Centaurs are only the largest members of the belt population with diameter estimates ranging be-

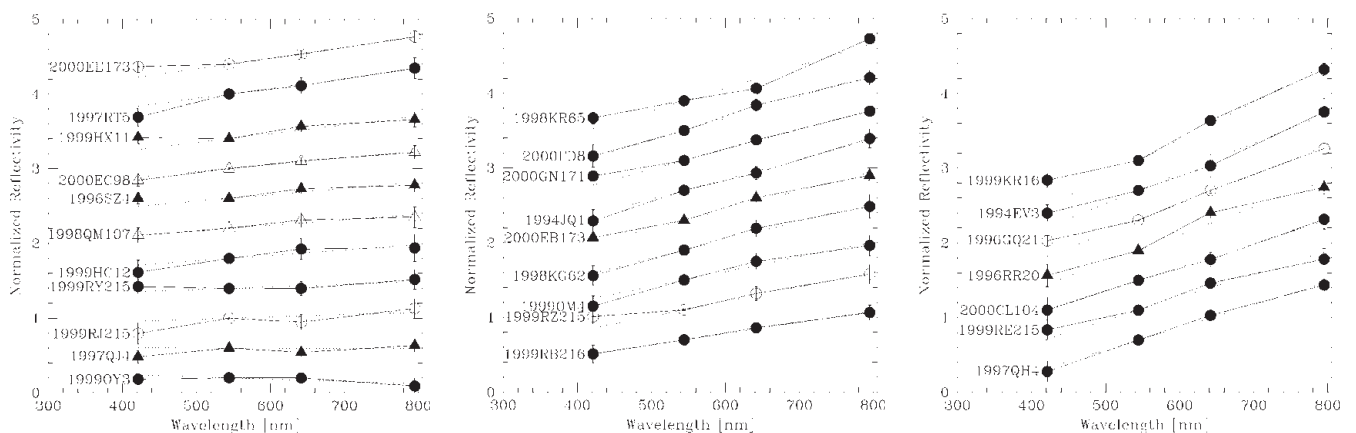


Figure 2: Photometric “reflectivity spectra” from BVRI magnitudes of TNOs and Centaurs. The three panels show the photometric “reflectivity spectra” of the first 28 objects observed with our programme. The relative reflectivity per photometric band (normalized to unity for V band) is plotted versus central wavelength of the filters used. It is a measure of the intrinsic reddening of the objects since the slope of solar spectrum is removed from the data. The broken lines indicate the numerical spectral gradient fits for the individual objects. These plots are very useful to check the consistency of the photometric data since “bad” measurements and intrinsic variability of the objects will result in noticeable deviations of the photometry from a “smooth” spectral slope in these “spectra”. If found, further investigations may be needed to clarify the nature of the scatter.

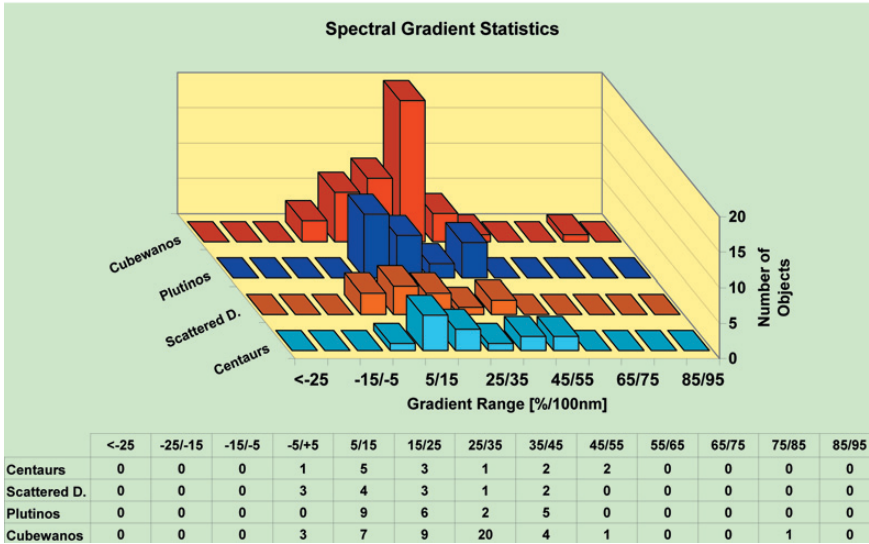


Figure 3: Spectral gradient histograms of the full sample of 96 objects in our analysis database. The histograms show the number of objects per spectral gradient interval for each dynamical class as given in the table at the bottom of the figure. The spectral gradients are calculated from the BVRI photometry of the objects.

tween 30 and 1200 km (assuming a low albedo of 4 per cent). Search programmes suggest a cumulative mass function with power exponent between 3.5 and 4. The albedo of less than 10 objects is coarsely determined: TNOs and Centaurs seem to be dark objects with albedo mostly around and below 10 per cent. Only Pluto, Charon and Chiron have high (around 50 per cent for Pluto and Charon) to moderate albedo, possibly caused by fresh ice due to intrinsic atmospheric activity (see below). The rotation period of more than 20 objects is measured with results ranging from 5 and 12 h (certainly biased since long periods are more difficult to measure). With the exception of Pluto and Charon, it is unclear whether the measured variability is due to body shape or surface reflectivity or both.

Until 2001 the taxonomic characterization of the population was based on a sample of ~ 50 TNOs and ~ 10 Centaurs, most of them observed with broadband colours in the visible wavelength range only. Nevertheless, colour-colour diagrams and reddening distributions provide a first glance of similarities and diversities in the surface taxonomy of the objects. A wide range of colours (in other words spectral gradients or 'reddenings') ranging from slightly bluer than the Sun ($\sim 5\%/100\text{nm}$) to extremely red ($\sim 50\%/100\text{nm}$) in the visible wavelength range is found in this sample. In the infrared, the photometric results indicate only minor reddening to neutral slopes of the surface reflectivity. For a finer analysis, the overall object sample contained some adverse culprits like bad number statistics for all dynamical classes, insufficient photometric accuracy of the data, incomplete wavelength coverage (7 objects had only 1 or 2 colours measured) and large differences in the results for the same objects obtained by different observers. It is thus not surprising that

different researchers arrived at different and partially contradictory conclusions, for instance a bimodal colour distribution versus a continuous one with 'outliers' in both scenarios. Through a Kolmogorov-Smirnov analysis of the sample it became clear that the identified colour populations among TNOs and Centaurs are at best to be considered as trends, but they lack clear statistical significance because of the low number of objects in the available sample.

Since formed in the outer solar nebula, TNOs and Centaurs should be made of icy and stony compounds. Except for the larger members that may have undergone constitutional modifications due to radioactive heating in their interior, and those that come closer to the Sun and thus get heated up in the surface layers, the original material remained unchanged in the body interior. Nevertheless, as outlined below, the surface layers of the bodies are all modified over the age of the solar system. N_2 and H_2O ices should be most abundant in TNOs and relatives, followed by CO , CO_2 , CH_4 and NH_3 . Signatures of N_2 , CO , H_2O , CH_4 and NH_3 ices are indeed found in spectra of Pluto/Charon. Water ice absorptions were detected in the Cubewano 1996 TO_{66} and the Centaurs 5145 Pholus and 2060 Chiron, objects that represent basically the fully colour range found in the total sample. The original 'stony' ingredients in TNOs and Centaurs should be primarily of silicate nature. Their detection, however, is extremely difficult since they may be covered completely with ice mantles. There is only one case, the Centaur 5145 Pholus, in which a very wide and close to marginal absorption feature (ranging from 0.6 to 1.6 μm) is tentatively attributed to silicates. The only other supportive argument for the presence of dust in these objects comes from the Centaur 2060 Chiron and of course their relatives, the short-period comets, i.e. through the

temporary dust coma seen around these objects.

Surface evolution scenarios: The red colour of TNOs and Centaurs is usually attributed to the effects of surface aging and darkening due to high-energy radiation and ion bombardment. Blue surface colours could be produced by major collisions through deposits of fresh icy material from the body interior or from the impactor. The estimated time scale for both types of colour resurfacing are of the order of 10 million years. The observed colour range can be modelled by computer simulations involving both effects. However, these results are unfortunately not discriminative for conclusions on the physical nature of TNO and Centaur surfaces. Resurfacing on much shorter time scales could happen due to ice re-condensation from a temporary atmosphere produced by intrinsic gas and dust activity. This process is quite efficient on Pluto and possibly Charon, but does certainly not work for all objects since crust formation may prevent the development of surface activity and/or the heat source in the bodies may not be strong enough to cause such activity.

ESO Large Programme on 'Physical Studies of TNOs and Centaurs'

Programme concept and history:

After a number of uncoordinated precursor programmes at ESO telescopes at the end of the last decade, a consortium of scientists (see the list of authors of this paper) proposed a comprehensive observing and analysis project to be performed within the framework of an ESO Large Programme: 'Physical studies of TNOs and Centaurs'. The project was accepted to be executed at Cerro Paranal and La Silla during ESO period 67 to 70, i.e. from April 2001 until March 2003. The main goal of the project is the development of a taxonomic classification scheme of these icy bodies in the outer solar system, the identification of evolutionary tracks and their relationships with dynamical classes, the exploration of the surface chemistry of the objects and its correlation with taxonomic classes. The proposed observing campaigns at the ESO Very Large Telescope (VLT) and the New Technology Telescope (NTT) comprise multi-colour broadband filter

photometry of 60–70 objects in the visible and about 25 objects in the near-IR wavelength range for the taxonomy analysis and low-dispersion spectroscopy in the visible and near-IR of about 15–20 objects each for the chemical studies. The ESO Programme Committee has allocated in total 242 hours of VLT time and 3 nights at the NTT for this Large Programme. The workhorse instruments for the proposed observations are FORS1 and ISAAC at the VLT Unit Telescopes 1 (Antu) and 3 (Melipal). Broadband photometry of some brighter targets is also conducted with SUSI2 at the La Silla NTT.

Observing modes and target selection: The majority of the photometry targets are observed in service mode (SM) at the VLT with the exceptions of brighter ones that are either imaged at the NTT or during spectroscopy runs in visitor mode (VM). Experience from previous programmes has shown that the SM targets have to be selected from amongst objects that allow safe detection in the fields of view of the instrument; in practice only objects with at least 2 observed oppositions appear to be ‘reliable’ to this respect. Less well observed targets have a high risk of being missed in the SM exposures that

typically happen about one year after the last object positions were measured. For the BVRI measurements we selected targets with V brightness of 22.5–24mag, while for JHK photometry the objects need to be brighter than 22.5mag in V. The SM targets are requested to be observed under clear to photometric dark sky conditions with seeing better than 0.8”. These constraints together with the chosen integration times guarantee a minimum signal-to-noise ratio (S/N) for the individual objects of 30–50 in BVRI and 20–40 in JHK. In terms of fulfilment of the observing requirements this part of our programme can be considered 100 per cent successful.

Observing strategies: The spectroscopy part of the programme is performed in visitor mode since the on-line detection of these slowly moving (typically 1–2”/h) faint targets in SM was considered risky and misidentifications may cause significant loss of observing time. The targets had to be selected amongst brighter objects, i.e. brighter than 22.5 mag in V for spectroscopy in the visible wavelength range and brighter than 20.5mag in V for the near-IR spectroscopy. Several of the targets had some BVRI colours measured from previous observations or other pro-

grammes. Nevertheless, quasi-simultaneous broadband photometry of the targets is taken during spectroscopy runs with the aim to verify the earlier results and – most importantly for the IR spectra – to cross-calibrate the continuum flux in the JHK bands of the objects as needed for the modelling of the spectra. Visible and near-IR spectroscopy runs are scheduled within a few days of each other in order to guarantee observations of the same object under similar phase angles. However, this scheduling usually did not allow us to correlate the rotational phase of the objects for the measurements in both wavelength ranges, mostly because for many objects the rotation parameters are not well known. The exposure times of the targets aimed for a S/N of about 3–10 per wavelength pixel element which through wavelength binning allowed improvements by a factor of 3–5. Given the faintness of the objects and the telescope/instrument capabilities, near-IR spectroscopy is the most time-consuming part of our programme even under favourable sky conditions, and typically 1 to 1½ nights of observing time are required per target. Unfortunately, the visitor mode observations so far have had an unexpectedly high ‘loss’ rate of about 25 per cent due to

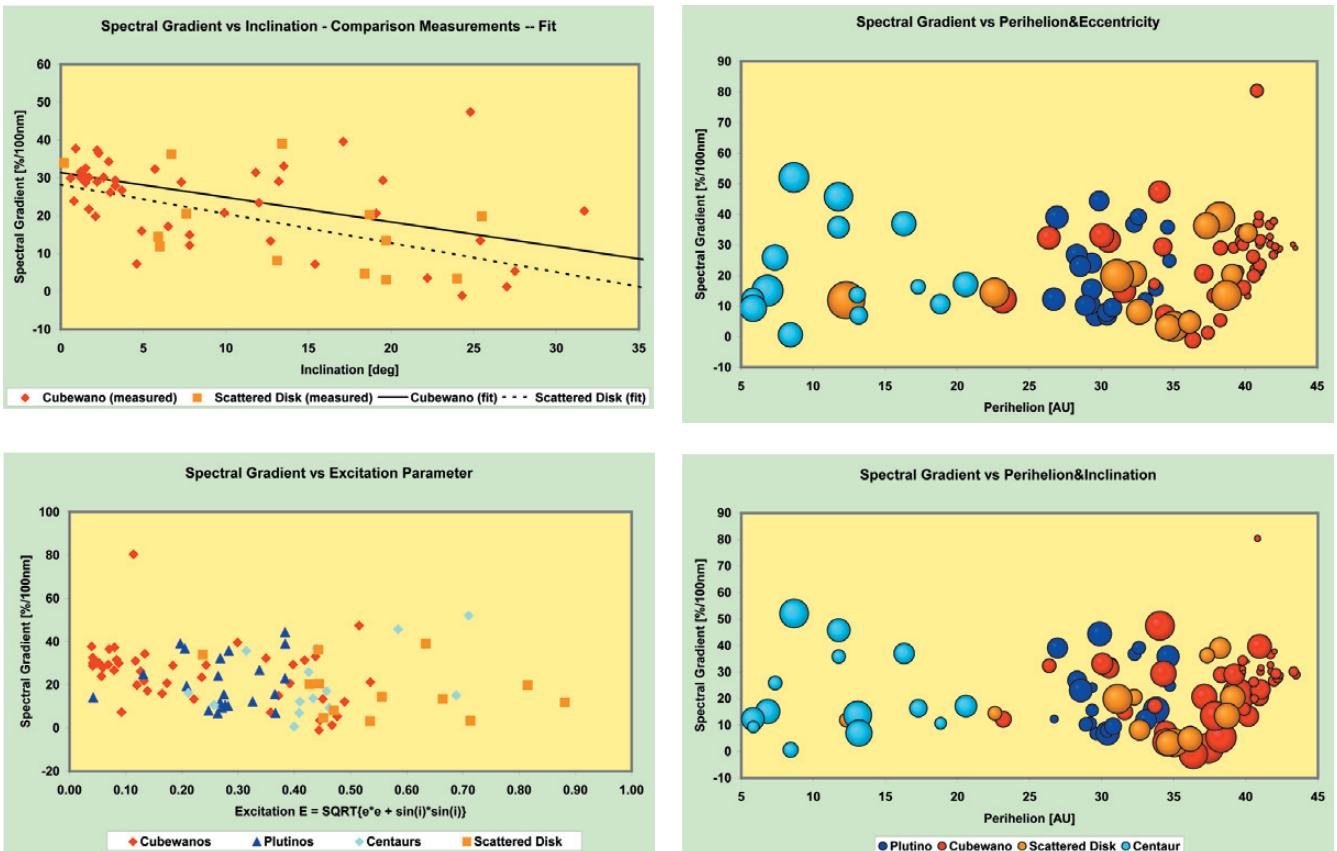


Figure 4: Spectral gradients versus orbital parameters. The plots show the measured (from BVRI photometry) spectral gradients of the objects versus orbital excitation E (lower left panel), inclination (upper left panel), and perihelion distance (upper and lower right panels). The bubble diagrams in the right panels use the orbital eccentricity (upper right) and the inclination (lower right) as size parameter of the bubbles, i.e. the smaller the bubble the lower the eccentricity and inclination, respectively. The colour coding of the dynamical classes is identical to Figure 2. The red Cubewanos beyond 41 AU mentioned in the text appear to cluster at the left end in the left panels and (as the tiny bubbles) to the right end in the right panels.

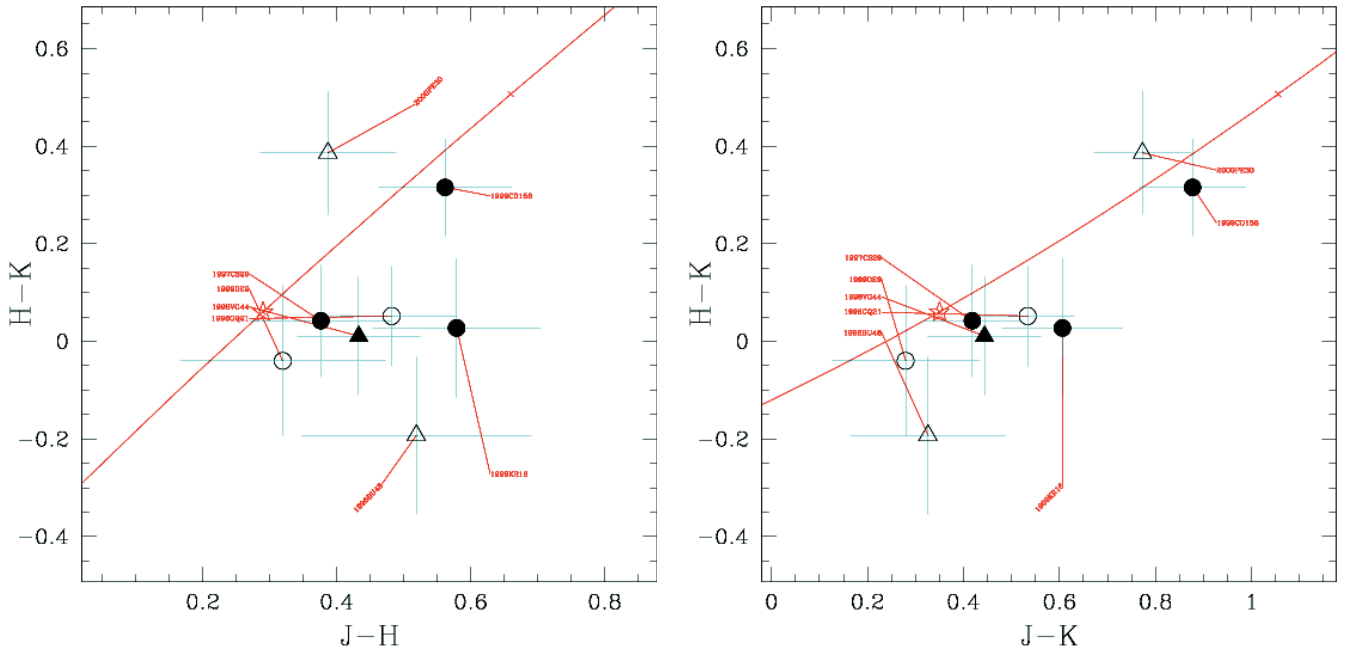


Figure 5: JHK colour-colour plots of the first 8 objects measured in the SM photometry part of our programme. $H-K$ versus $J-H$ is displayed in the left panel, the right one shows $H-K$ versus $J-K$. For explanations of symbols and lines see Figure 1. The objects are identified with small labels at the symbols.

bad sky conditions and some technical problems. Additional overheads and further time loss due to weather are caused by the need to cross-calibrate the spectra in the three near-IR wavelength regions through JHK absolute photometry. The availability of dispersive optics covering more than one near-IR band at lower spectral resolution could have resulted in additional benefits and higher efficiency for our programme.

Data reduction: The basic data reduction products of the photometry are absolute broadband filter magnitudes in BVRI and JHK, filter colours and spectral gradients. As side results astrometric positions and a search for satellites around the prime targets are performed (so far without success). The magnitude (equivalent to sizes), colour and gradient data are correlated with each other and with orbital parameters to associate and explore taxonomic classes and their colour properties through statistical methods. This exercise is applied to our database alone and to an even larger dataset merging our results with those published in the literature. The spectra are reduced to relative reflectivity units that allow us to determine spectral gradients and to identify absorption features that may be indicative for the surface chemistry. Each spectrum covering a wider wavelength range is modelled through a Hapcke reflectance modelling code to constrain and, if possible, to quantify the surface chemistry of the targets. In a final phase of the project it is planned to correlate spectral properties with the photometric taxonomy of the objects.

Status of the programme: By the end of 2002, about 90 per cent of the

observations had been conducted and about 60 per cent of the data reduction and analysis phase is performed. Table 1 shows the number of objects observed per dynamical class (Cubewano, Plutino, SDO, Centaur) and observation type (BVRI and JHK photometry, visible and near-IR spectroscopy). Up to now, the photometry worked out as planned, while the spectroscopy suffered from time losses (as explained above). Since the object selection for SM observations had to be done months in advance, some of our targets have been observed by other groups in the meanwhile, and despite all efforts, duplication of observations turned out to be unavoidable. A few targets were selected on purpose for repetition of certain types of observations in order to allow cross-checks of our results with those of other observers and to address specific unsolved questions related with the objects. The most striking constraint causing duplication is the fact that the sample of near-IR targets accessible with standard instruments at modern 8–10-m class telescopes is rather limited (~ 30 objects up to now).

Highlights from the First Results

The results outlined in this summary are obtained from data collected during the first year of this ESO Large Programme. They are described in greater detail in various papers that are already published (Barucci et al., 2002, *A&A* 392; Boehnhardt et al. 2002, *A&A* 395) or will be published soon (Dotto et al., 2003, *Icarus*, in press; Lazzarin et al. 2003, *AJ*, in press). Another three papers with results from Period 69 are in preparation for submission to scientific journals in early 2003.

BVRI colour-colour-plots and spectral gradient histograms: The database used here contains 96 objects compiled from our programme (28) and from published data. The colour-colour-plots and photometric “reflectivity spectra” of the 28 objects measured by our programme in Period 67 are displayed in Figures 1 and 2, respectively. The colour-colour plots (Fig. 1) show that the objects follow – with some scatter – the lines of constant reddening in BVR colours, but they start deviating in the transition re-

Table 1. Physical studies of TNOs and Centaurs: Number of objects observed/reduced per dynamical class (status: end 2002).

Object class	BVRI	JHK	vis.spec.	IR spec.*
Cubewanos	25/15	7/4	1/1	0/0
Plutinos	19/10	7/4	5/4	4/3
Scattered Disk	13/7	6/5	3/2	3/2
Centaurs	9/7	6/5	6/6	5/4
Total	66/39	26/18	15/13	12/9

*About 30 % of the object spectra are incomplete, i.e. JHK bands are not fully covered.

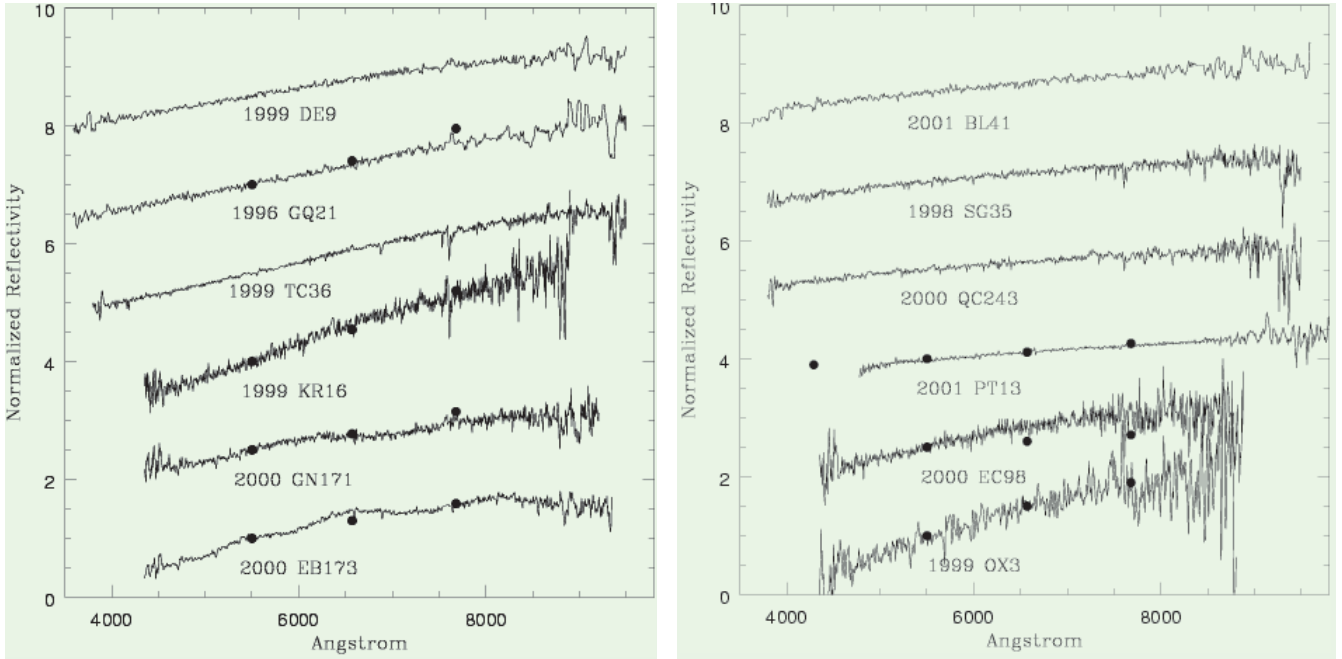


Figure 6: Visible Reflectivity spectra of TNOs and Centaurs. The spectra of TNOs are displayed in the left panel, those of Centaurs in the right one. The spectra are shifted in Y direction for clarity. The dots represent the respective results from quasi-simultaneous photometry of the objects taken during the spectroscopy runs.

gion to the near-IR. The latter is a consequence of the slope change seen in the spectra of red to very red objects beyond 750 nm. The reddening distribution seems to be continuous without a clear indication for a bi-modality as announced by other groups using smaller datasets. In the spectral gradient histogram of Figure 3 all 96 objects are used and sorted for each dynamical class in the same gradient bins of width corresponding to the averaged uncertainty of the data. With one exceptions (1994 ES₂) the spectral gradients of all objects fall between -5 and $55\%/100$ nm. Outliers in previous datasets turned out to be artefacts, most likely due to observations and data reduction (blends of background objects) or unusual object behaviour (for instance 1994 EV₃ shows rapid and large-amplitude variability that mimics unusual colours even in short-term photometric filter sequences as identified through our programme). The Cubewanos show a pronounced peak for spectral gradients between 25 and 45 $\%/100$ nm that is caused by a population of red objects in circular and low inclination orbits beyond 41 AU. At least for the Plutinos, and possibly also for Centaurs and SDOs, the distribution of spectral gradients in the visual wavelength region seems to be distinctly different from those of the Cubewanos.

Correlations with orbital parameters: In Figure 4 we show the measured photometric spectral gradients versus orbital excitation E , inclination and perihelion distance of the objects. The excitation parameter is defined as $E = (e^2 + \sin^2(i))^{1/2}$ with e and i as eccentricity and inclination of the orbit,

respectively. E is an estimate for the velocity of the object with respect to another one at the same distance, but in circular orbit in the Ecliptic, and it might thus be related to the collision velocity and/or the collision probability. The plots of the spectral gradients versus E and i suggest a correlation between surface colour and collision history of the objects, since the range of spectral gradients increases with increasing excitation parameter E and decreases with decreasing inclination. On the other side, the plot of the spectral gradients versus perihelion distance shows a clustering of very red Cubewanos in circular and Ecliptic orbits beyond ~ 41 AU. The peak for the Cubewanos in the spectral gradient statistics of Figure 3 is caused by exactly this group of objects. Moreover, for objects with perihelia between ~ 36 and 40 AU the width of the reddening range seems to increase the closer the object approaches the Sun. At present, these trends are not yet fully established since more objects need to be included for statistical reasons. However, if the trends can be confirmed, they would argue for different reddening scenarios, i.e. the trends with excitation and inclination for the balance between space weathering and collision resurfacing on one side and the trend with perihelion distance for the balance between space weathering and intrinsic activity on the other side. Most puzzling is the group of red Cubewanos beyond 41 AU and there is no easy explanation for their existence at present.

JHK colours: While at visible wavelengths a certain reddening range seems to be continuously populated, a

preference for neutral colours is found among the near-IR spectra of the objects – see Figure 5. Only 2 objects are definitely redder than the Sun. Whether the red objects are members of a second colour population can easily be questioned. The overall interpretation of the visible to near-IR colour range argues for only minor colour changes in the infrared part of the spectra, but for a significant and very wide absorption of variable depth for many TNOs and Centaurs in the visual wavelength range. This implies that the observed reddening in BVRI is in fact the long-wave wing of a wide absorption feature from a yet unknown chemistry that extends beyond the visible region well into the UV.

Visible spectra: The spectra of TNOs and Centaurs observed in the visible are mostly featureless and show constant (though different) slopes at wavelengths below ~ 750 nm (Fig. 6). At larger wavelength a continuous gradient change towards smaller slopes is observed in the red objects. With one exception (possibly caused by rotation effects in the photometry) the spectral gradients obtained from spectra are in good agreement with the photometric ones. It came as a surprise that wide absorption dips were found in the visible spectra of two Plutinos, 2000 EB₁₇₃ and 2000 GN₁₇₁, taken in April 2001 (see Fig. 7). The absorption features are centred around 600 and 730 nm for 2000 EB₁₇₃ and at 725 nm for 2000 GN₁₇₁. There are two very puzzling aspects with these detections: (1) The features were not confirmed with spectra taken about one year later (see Fig. 7); this would argue for a non-uni-

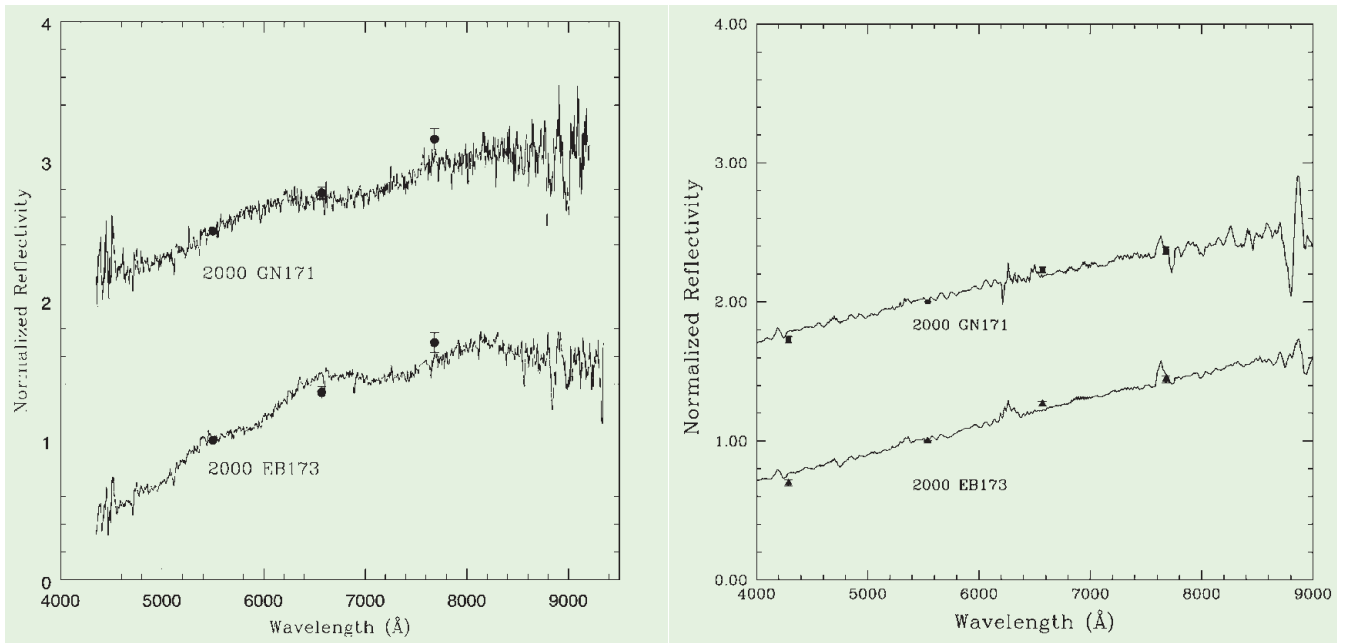


Figure 7: Two “puzzling” Plutinos: reflectivity spectra of 2000 EB₁₇₃ and 2000 GN₁₇₁. The reflectivity spectra of both objects show shallow and wide absorption features during one observing epoch (left panel), but a straight featureless slope during a second observing run about one year later (right panel). The dots and triangles in the panels indicate the corresponding ‘broadband’ reflectivity from quasi-simultaneous BVRI filter photometry of the objects.

form distribution of the absorbing material on the surface of the objects. (2) Features resembling the absorptions in these two Plutinos and identified in other solar system bodies and in lab experiments are produced by silicate material on asteroids that was exposed to long-term aqueous alteration on the surface. A similar scenario in the extremely cold and icy environment of the outer solar system obviously poses some problems. The answer to this puzzle calls for a systematic study of the objects by rotation-phase resolved spectroscopy, and, if confirmed, it will

have a great impact on our understanding of the physical nature of these bodies at the edge of the planetary system.

Near-IR spectra: We have found water ice absorption in H and K band spectra of 1 TNO and 3 Centaurs (see for instance the 2001 PT₁₃ spectrum in Figure 8). No features are seen in the spectra of other objects in our sample. For 2001 PT₁₃, a non-uniform water ice distribution on a large scale is concluded from the existence and absence of the absorption features in the spectra measured at two different epochs. The

model fits to the combined near-IR and visible spectra use a radiative transfer code with simple geographical mixtures of organics, minerals and ices. The steep slopes in the visible require the admixture of Tholins or kerogene in the model fits. Nevertheless, despite the decent match that is achieved between the observed spectra and the radiative transfer model results, at present our conclusions are limited. On one hand, water ice seems to be present in

Conclusion and Outlook

these distant bodies; however, on the other hand, the identification of further surface materials as well as quantitative estimations are difficult because of the quality of the data fits and the existence of multiple model solutions for each spectrum.

The ESO Large Programme on the physical studies of TNOs and Centaurs is now approaching the end of its assigned period for the observations, and it is a little more than half way through the data reduction. The analysis of the results and model interpretation will certainly continue for another year beyond the official end of the observing programme. With the data from this programme it has been possible to identify the first taxonomic group in the Edgeworth-Kuiper Belt, the cluster of red Cubewanos beyond 41 AU, and to get clear indications of resurfacing effects on TNOs and Centaurs. At the moment, the observed results appear to be somewhat contradictory to each other and a synoptic picture for their interpretations has not yet evolved. Water ice seems to be abundant in these objects; however, the identification of other surface ice features appears to be a difficult task. Spectra of two Plutinos may have provided the first glance of stony material, and if so, they contribute yet another puzzle with the potential to drastically change our view of these icy worlds in the outer solar system.

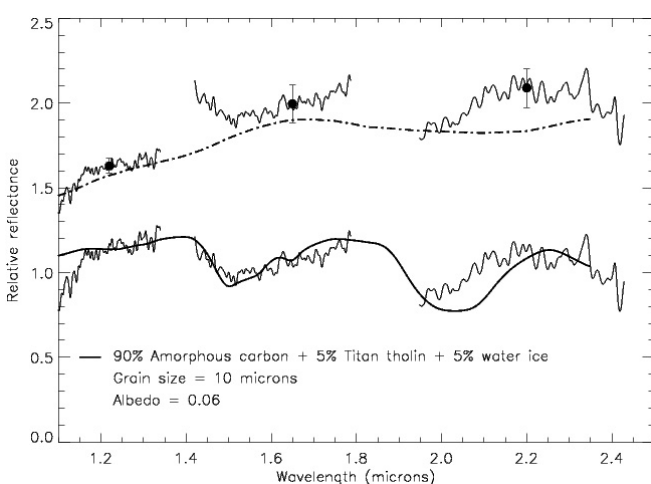


Figure 8: Near-IR spectrum of the Centaur 2001 PT₁₃. The plot shows the near-IR spectrum of the object on 10/9/2001 (upper spectrum) and on 8/10/2001 (lower spectrum). The continuous and broken lines show model fits to the observed spectra using the material mixture as indicated in the figure insert. The dots indicate the reflectivity from quasi-simultaneous broadband JHK photometry of the object.